2019

Archetypes of human cognition defined by time preference for reward and their brain correlates: An evolutionary trade-off approach

Giorgia Cona

Loren Kocillari

Alessandro Palombit

Alessandra Bertoldo

Amos Maritan

See next page for additional authors

Authors
Giorgia Cona, Loren Kocillari, Alessandro Palombit, Alessandra Bertoldo, Amos Maritan, and Maurizio Corbetta

NeuroImage 185 (2019) 322–334

Contents lists available at ScienceDirect

NeuroImage

journal homepage: www.elsevier.com/locate/neuroimage

Archetypes of human cognition defined by time preference for reward and their brain correlates: An evolutionary trade-off approach

Giorgia Cona [a,f,1], Loren Koçillari [b,f,1], Alessandro Palombit [c,f], Alessandra Bertoldo [c,f], Amos Maritan [b,f,2], Maurizio Corbetta [d,e,f,*,2]

[a] Department of General Psychology, University of Padua, Italy
[b] Department of Physics, University of Padua, Italy
[c] Department of Information Engineering, University of Padua, Italy
[d] Department of Neuroscience, University of Padua, Italy
[e] Departments of Neurology, Radiology, Neuroscience, Washington University School of Medicine, Saint Louis, USA
[f] Padova Neuroscience Center (PNC), University of Padua, Italy

ARTICLE INFO

Keywords:
Evolutionary psychology
Brain
Multi-objective optimization
Reward
Delay discounting task
Self-control
Functional connectivity
Human connectome project

ABSTRACT

Biological systems carry out multiple tasks in their lifetime, which, in the course of evolution, may lead to trade-offs. In fact phenotypes (different species, individuals within a species, circuits, bacteria, proteins, etc.) cannot be optimal at all tasks, and, according to Pareto optimality theory, lay into a well-defined geometrical distribution (polygons and/or polyhedrons) in the space of traits. The vertices of this distribution contain archetypes, namely phenotypes that are specialists at one of the tasks, whereas phenotypes toward the center of the geometrical distribution show average performance across tasks.

We applied this theory to the variability of cognitive and behavioral scores measured in 1206 individuals from the Human Connectome Project. Among all possible combinations of pairs of traits, we found the best fit to Pareto optimality when individuals were plotted in the trait-space of time preferences for reward, evaluated with the Delay Discounting Task (DDT). The DDT measures subjects' preference in choosing either immediate smaller rewards or delayed larger rewards. Time preference for reward was described by a triangular distribution in which each of the three vertices included individuals who used a particular strategy to discount reward. These archetypes accounted for variability on many cognitive, personality, and socioeconomic status variables, as well as differences in brain structure and functional connectivity, with only a weak influence of genetics. In summary, time preference for reward reflects a core variable that biases human phenotypes via natural and cultural selection.

> "Pleasure is the only thing worth having a theory about," he answered in his slow melodious voice. "But I am afraid I cannot claim my theory as my own. It belongs to Nature, not to me. Pleasure is Nature's test, her sign of approval".
>
> (Oscar Wilde, The Picture of Dorian Gray)

According to natural selection, biological systems coevolve to maximize their fitness function, resulting in optimal phenotypes. However, when facing complex environments, systems carry out multiple tasks, and all of these tasks contribute to fitness. Hence a fundamental trade-off: As systems cannot achieve optimal performance in all tasks, becoming specialists in one set of tasks necessarily leads to a reduction of performance in a different set of tasks.

A recent paper (Shoval et al., 2012) applied a theory typically employed in engineering and economics - the Pareto Optimality - to identify evolutionary trade-offs in biological systems. The Pareto Optimality approach has been successfully applied to animal morphology (Shoval et al., 2012; Szekely et al., 2015), animal behavior (Gallagher et al., 2013), cancer (Hart et al., 2015), ammonite shells (Tendler et al., 2015), bacterial and single cells gene expression (Thøgersen et al., 2013;

* Corresponding author. Department of Neuroscience, Clinica Neurologica Azienda Ospedaliera, University of Padua, Via Giustiniani 5, 35128, Padova, Italy.
E-mail address: maurizio.corbetta@unipd.it (M. Corbetta).
[1] Equal contribution first author.
[2] Equal contribution senior author.

https://doi.org/10.1016/j.neuroimage.2018.10.050
Received 21 May 2018; Received in revised form 5 October 2018; Accepted 18 October 2018
Available online 21 October 2018

Korem et al., 2015), biological circuits (Szekely et al., 2015), and more recently to the structure of polymorphisms (Sheftel et al., 2018), and to *Escherichia coli* proteome (Koçillari et al., 2018).

The starting point of the Pareto Optimality approach is to define the space of traits, or *morphospace*, where traits represent physical features such as body mass, longevity, brain size etc, and species are usually data points in the morphospace.

The Pareto Optimality theory predicts that if traits are likely to show trade-offs, then phenotypes will be enclosed into a well-defined geometrical domain of this morphospace called *polytope* (e.g., a segment, a triangle, a pentagon or other low dimensional polygons/polyhedra …). This polytope will include the phenotypes that have found the best possible trade-off solutions among different traits, and will represent the *Pareto front* solution. In the absence of trade-offs, phenotypes will be instead distributed in an uncorrelated cloud of points in the morphospace.

The position of a given phenotype inside the Pareto front distribution is informative of its evolutionary strategy. Specifically, the vertices of the polytope contain the *archetypes*, namely the phenotypes that have traits leading to the maximal performance in one of the tasks and minimal performance in the competing tasks. Other key biological traits related to that task will be then maximally expressed or 'enriched' near that archetype, and minimally enriched near the other archetypes. By 'enrichment' we mean the expression of maximal or minimal scores on a particular trait in a cluster of subjects.

Phenotypes that fall in the middle of the polytope are *generalists*, i.e. showing average performance in those tasks that define the trait space. In the case of two competing tasks, the phenotypes fall on a line segment in the morphospace, whereas for three tasks the phenotypes fall into a triangle. Four tasks would result in a tetrahedron distribution, and so on. Notably, this analysis is data-driven since it is the distribution of the data to indicate which tasks show trade-offs.

An example of the application of Pareto optimality is the study by Szekely et al. (2015). The authors found that species of mammals and birds fall within a triangular Pareto front distribution when they are projected in a morphospace created by the variables longevity and mass. The vertices of this triangle represent three archetypes. Specifically, large animals with high longevity (whales being the archetype); small animals with high longevity (bats); and, small animals with low longevity (mice). All other species, including humans, fall in between. Importantly, through enrichment analysis, it is possible to show that these traits are related to other traits that account for their evolutionary fitness. For instance, small animals with low longevity tend to have high fertility and tend to be preys (mice); conversely, small animals with high longevity have lower fertility, but also tend to be predator (bats).

In this study we test the predictions of Pareto optimality theory to human cognition and behavior by analyzing data from the Human Connectome Project (HCP) that includes a wealth of cognitive, personality, health, socio-economic status, and brain measures (Van Essen et al., 2013). Specifically, in a large population of subjects, the theory predicts that some individuals will excel at some tasks at the expense of others (i.e. *archetypes)* while most subjects (i.e. *generalists)* will show average performance.

The trade-offs in cognitive tasks predicted by the Pareto optimality theory are not a given. In fact, the well established theory of general intelligence, or *g-factor*, posits a positive correlation among a large number of cognitive tasks (Spearman, 1904). While human intelligence may embrace more than sixty specific cognitive abilities, the *g factor* is common to all of them (Carroll, 1993; Colom et al., 2006), explaining large amount of variance (~45–50%) across test scores in large samples of healthy subjects (Austin et al., 2002; Floyd et al., 2009).

First, we asked if neuropsychological or behavioral scores distribute according to Pareto Optimality theory. We focused on triangular shaped distribution. In principle, other polygons or polyhedrons in higher dimensional space might exist, but, based on prior evolutionary studies (Shoval et al., 2012; Gallagher et al., 2013; Szekely et al., 2015; Tendler et al., 2015; Koçillari et al., 2018) the focus was on triangular solutions.

Second, after finding the combination of pairs of traits where data point distribution best fit a triangular distribution, we identified those traits that characterized the three archetypes. We considered not only cognitive, but also affective, personality, and socio-demographic measures. Based on this enrichment analysis, we inferred the competing human evolutionary strategies.

Third, we identified differences among archetypes in brain structure (volume, gray matter, etc.), and function (resting state functional magnetic resonance imaging rs-fMRI connectivity).

Finally, we explored the influence of genetics on archetype variability. Specifically, we asked if behavioral scores on the identified tasks were more concordant in monozygotic versus dizygotic twin pairs.

This report will focus on the best triangle in the morphospace of traits of the HCP dataset. This triangle includes individual scores on two measures of the Delay Discounting Task (DDT). The DDT measures the tendency to opt either for immediate smaller rewards or delayed larger rewards (Green and Myerson, 2004; Kirby and Marakovic, 1996). This task assumes that the subjective value of a reward (e.g., money) is increasingly discounted from its nominal amount as a function of the delay until reward reception. Discounting is a pervasive phenomenon in decision making shared by humans and animals (Peters and Büchel, 2011). The DDT is a sensitive measure of the ability to wait for a reward (time preference) as well as impulsivity and self-control processes (Kirby et al., 1999; Mobini et al., 2007). In the context of Pareto Optimality, the vertices of this triangle contain individuals that use different strategies to discount reward in time. Interestingly, these groups enriched on a variety of other cognitive, behavioral, socio-economic, and health features, and differed on measures of brain structure and function. However, genetic influence was modest. Therefore, strategies for discounting reward represent phenotypes that have developed under evolutionary and/or cultural pressures to adapt to our environment.

1. Materials and methods

1.1. HCP dataset

We analyzed the public data release of the WU-Minn Human Connectome Project (HCP) consortium (Van Essen et al., 2013), which includes 1206 healthy young adults, from families with both twins and non-twin siblings. The current sample was obtained from the March 2017 data release (1200 Participants; http://www.humanconnectome.org). The database consists of behavioral measures (e.g., cognitive, personality), socio-demographic measures, and high-resolution 3T MRI imaging data.

Some data are restricted due to subject privacy (e.g. twin or smoking status etc). The HCP subjects include 168 Monozygotic twin pairs, and 103 Dizygotic twin pairs. The behavioral database consists of tests that are part of the NIH Toolbox battery and of several Non-Toolbox behavioral measures (see Supplementary Material for a detailed description).

For each subject, we also obtained the brain volumes from the Freesurfer software and analyzed them by voxel-based morphometry. They consist of continuous features and are normalized with respect to intracranial volume.

1.2. Pareto Optimality Inference method

The Pareto Optimality analysis is based on the following assumptions:

1) Subjects are assigned a set of continuous traits ν, which in our case correspond to measures of cognitive, personality, socio-demographic, and brain features.
2) Subjects can perform *k*-tasks simultaneously. Tasks are in trade-off with each other, and each of them is assigned a performance

function $P_k(\nu)$ that quantifies the ability of a given subject to perform that task.

3) The performance of a k-task is maximal near the vertex ν^i, and it decreases monotonically with the Euclidean distance from the vertex as follows $P_i(d^i(\nu)) = P_i((\nu - \nu^i)^T M(\nu - \nu^i))$, where i = 1, …,k and M is a positive-definite matrix (M = **I** for Euclidean metric).
4) Natural selection induces subjects to maximize their fitness function, defined as an increasing function of all the performances $F(P_1(\nu)…P_k(\nu))$. In the case with tasks in trade-off, it results in a multi-objective optimization problem that has as optimal solutions those points that satisfy $\nu = \sum \theta_i \nu^i$ (with i = 1, …,k), where $\theta_i = \frac{\partial F}{\partial P_i}\frac{\partial P_i}{\partial d_i} / \sum_j \frac{\partial F}{\partial P_j}\frac{\partial P_j}{\partial d_j}$ and $\sum \theta_i = 1$ which define Pareto fronts (or polytopes) in the space of traits (Shoval et al., 2012). The points nearest each vertex of the polytopes correspond to specialized individuals with the highest performances in that task, i.e. *archetypes,* and lowest in the others.

In our analysis, we focused on identifying the best-shaped polytope that encloses the data points in the space of traits starting from a triangular Pareto front distribution (Bioucas-Dias, 2009).

As compared with other classical clustering methods (k-means, Gaussian Mixture models, Latent Class Analysis), Pareto Optimality approach differs as it identifies the vertices (rather than centroids) of a distribution. Clustering and Pareto analysis are indeed both able to find centroids, but in a complementary way, since the former is sensible to local density inside the distribution, while Pareto is mainly sensitive to the external shape (the external perimeter) of distributions, also called convex hulls (for further comparisons between the Pareto method and clustering methods see Hart et al., 2015).

Pareto analysis and enrichment analysis, as described below in this section, were run using the software package ParTI: (https://www.weizmann.ac.il/mcb/UriAlon/download/ParTI).

The first step in our analysis was projecting for each pair of behavioral measures the 1206 participants' data points in a two-dimensional space. We considered measures related to each cognitive and performance domain (e.g., fluid intelligence, memory, spatial orienting, self-regulation, strength, dexterity etc. (see Supplementary Materials). After removing redundant, ordinal measures or measures with too few observations, we considered a subset of 25 traits and we combined them in pairs of cognitive and performance-related traits, resulting in 300 possible combinations (see Supplementary Materials for details on the measures).

As a second step, we checked if the distribution of points obtained for each combination of pairs of traits fits a triangular shape (Mørup & Hansen, 2012). The statistical significance of each potential triangle was tested with the triangularity test (the t-ratio test). The t-ratio stands for the fraction between the area of the triangular hull defined through the Sisal algorithm (Bioucas-Dias, 2009), and the area of the best convex hull that encloses the cloud of data points. T-ratio values close to 1 indicate a better fit of the cloud of points to a triangle. For each triangular-shaped distribution we tested the robustness of the triangles by comparing the t-ratio of the original distribution with the t-ratio derived from n-null distributions derived from 1000 random permutations of the values of the data points while preserving the same cumulative distribution function (CDF) for a given set of values. This corresponding p-value defines the fraction of times the null t-ratios are lower than the empirical t-ratio, and statistical significant p-values should score under 5% of times ($p < 0.05$). We performed this analysis in the space of each of the 300 combinations of traits, and in each case we found a p-value for the triangular-hull. A correction for multiple comparisons was applied to all the p-values through the False Discovery Rate (FDR) method.

To further assess the validity of a triangular Pareto distribution, we measured the fraction of variance accounted for (across subjects) as a function of the number of vertices (2–6) of the possible polygons.

1.3. The delay discounting task (DDT)

Since the best Pareto front solution was observed in the morphospace created by two measures of the Delay Discounting Task (DDT), here we briefly describe the DDT. All subsequent analyses (enrichment, structural and functional brain features, heritability) will be carried out on the distribution of data points derived from the combination of two measures of the DDT.

In the DDT, participants were asked to choose between two options on each trial: a smaller amount of money to be given immediately vs. a larger amount of money given at a later point in time. Participants made choices for each of 6 possible delays (1 month, 6 months, 1 year, 3 years, 5 years, and 10 years), and for two 'reference' delayed amounts that were kept constant ($200 and $40,000). The amount available immediately was instead adjusted after each choice in order to determine the amount judged subjectively as equivalent to the delayed amount. If the participant chooses the immediate amount, then the immediate amount was reduced on the next trial, whereas if he/she choose the delayed amount, then the immediate amount was increased.

For each combination of amount of delayed reward and time delay, participants were asked to make 5 choices, and the value that would have been used for the immediate amount in the 6th choice was used as the indifference point. The indifference point represents the point where an individual is equally likely to choose a smaller reward earlier (e.g., $50 immediately) versus a larger reward later on (e.g., $200 in 1 month).

The Area under the curve (AUC) for each of the two reference amounts ($200 and $40,000) was computed based on the indifference points and ranges from 0 (maximum discounting) to 1 (no discounting) (Myerson et al., 2001).

The AUC measures of the DDT are considered a reliable indicator of self-control in cases of lower discounting rate (i.e. preference for larger delayed rewards), and impulsive behavior in cases of higher discounting rate (i.e. preference for smaller earlier rewards) (Kirby et al., 1999; Mobini et al., 2007). Although the rewards are hypothetical, there is a good correspondence with real rewards (Lagorio and Madden, 2005).

Based on the processes involved in the DDT, the three vertices ('archetypes') of the Pareto front triangle identify three optimal strategies to deal with discounting reward in time.

1.4. Validation of Pareto front solution

Even though the triangularity test examines the statistical significance of the obtained Pareto front solution against a null distribution through permutation tests, we also ran additional validation analyses.

In one analysis, we performed a split-half replication: we ran the Pareto analysis separately on two random independent smaller samples of the HCP data set (n = 559 and n = 560 subjects, respectively), taking into account all 300 possible combinations of pairs of the 25 traits. This was done to ensure that the Pareto Front solution obtained from Pareto Optimality Inference method was robust, i.e. significant in two independent samples.

We also asked whether the obtained Pareto front solution was robust to gender and race. In one analysis, two samples of subjects were created based on gender: Males (549 subjects) vs. Females (649 subjects). In the second analysis, three groups of subjects were compared: Asian-Nat. Hawaiian-Other Pacific (n = 67 subjects) vs. Black or African American (n = 192 subjects) vs. White (n = 883 subjects).

1.5. Enrichment analysis of the archetypes

According to the Pareto Optimality theory, the vertices of the triangle identify specialists that express different traits to the maximum (or minimum) extent, and that according to the theory are in trade-off. If Pareto theory is correct, then, other traits (i.e., enriched features) should be maximal or minimal in those specialists, and performance on those traits should decline (or rise) as a function of the distance from that

archetype.

To identify traits that enrich, we first divided the distribution of individual scores in bins and then analyzed, for each trait, the change of the mean value of that trait across the bins of the polytope, normalized with respect to the mean value of the given trait for the whole distribution. For simplicity, we binned the Pareto front three times, each time starting from one of the three vertices, into n bins. To make the analysis statistically valid in terms of sample size, we constrained each bin to contain the same number of participants. This procedure was repeated systematically by varying the number of bins between 8 and 15. A higher number of bins leads to higher statistical fluctuations in the density analysis. Features could be discrete or continuous. For continuous variables, we computed the ratio among the mean value at all bins and the mean value of the entire triangle. We plotted this ratio as a function of the n-th bin. For discrete features, we first booleanized them (i.e. a value 1 was given if the participant had the given feature, 0 otherwise), then we treated them as continuous variables.

Enriched features were validated if they passed the p-value test based on the hyper-geometrical distribution (Hart et al., 2015) and corrected for FDR test. This test measures the probability that the mean value of a trait is maximal/minimal in the bin closest to a given vertex. The robustness of the enrichment was assessed by performing a null-test, namely a random permutation of the values of the traits among the different bins.

Features belonging to four main domains were separately analyzed: 1. Cognitive, Physical and Sensory traits (1119 subjects and 46 measures); 2. Discrete traits of Personality, affective behavior, substance abuse, socio-demographic features (1123 subjects, 40 measures); 3. Continuous traits of Personality, affective behavior, substance abuse, socio-demographic background (1123 subjects, 70 continuous measures); 4. Structural brain measures (1105 subjects and 56 measures).

Structural brain measures (n = 56) included volume of cortical gray matter, white matter, and volume of anatomical regions in the right and left hemisphere (e.g. right and left hippocampus, thalamus, etc.) segmented in Free Surfer. Before running the enrichment analysis, the measures were first normalized per intracranial volume.

1.6. Resting-state functional connectivity analysis

To characterize differences in functional connectivity among different archetypes of significant Pareto front solution, we analyzed resting state functional connectivity (FC) from R-fMRI as available in the HCP data set.

Subjects. Three-hundred healthy subjects (172 F, age: 29 ± 3y) were selected from the 1200-subject release HCP dataset, considering, for each archetype, 100 subjects with minimal Euclidean distance from each archetype vertex of the Pareto distribution. This sample size was selected because it was similar to the average sample size of the binning analysis for feature enrichment.

Imaging Data. The HCP imaging protocol included up to four 15-min runs of resting state fMRI (60 min total), divided in two imaging sessions (TR = 720 ms, isotropic voxel-size 2 mm) and structural images, made available as data packages with pre-defined processing options, for more details refer to the study by Glasser et al. (2013). In this analysis, we employed minimally pre-processed fMRI time series from surface space defined and registered by means of a Multi-modal surface alignment method (MSM-All, (Robinson et al., 2014)) with minimal smoothing (surface and volume based 2 mm spatial smoothing) and de-trending. Moreover, FIX-ICA (Salimi-Khorshidi et al., 2014) denoised data was employed as available from HCP public repository to reduce motion-related confounds (Marcus et al., 2011).

Data Processing. Available denoised rs-fMRI time-series were signal averaged based on the functional parcels defined from the Gordon-Lauman scheme (2014) for cortical regions, and a volume based segmentation (Fischl et al., 2002) for subcortical regions (Cerebellum, Putamen, Pallidum, Ventral Diencephalon, Thalamus, Caudate, Amygdala, Hippocampus, and Accumbens in each hemisphere and Brainstem). Parcellated rs-fMRI time series were Pearson cross-correlated and Fisher r-to-z transformed ($z = 0.5 * \ln[(1 + r)/(1r)]$, with r the estimated Pearson linear correlation coefficient at edge-level (Hlinka et al., 2011) to obtain for each subject and run a FC matrix across 352 brain regions (Smith et al., 2011). We discarded rs-fMRI runs that included more than 30% of motion corrupted volumes. Framewise Displacement (FD) was employed to identify the motion-corrupted volumes as it indexes bulk head movements across consecutive volumes (Power et al., 2014) from the volume realignment parameters (motion correction). Since the available rs-fMRI data were previously pre-processed with FIX-ICA denoising, we relaxed the threshold for motion-corrupted volumes to FD > 0.5 mm as compared to previous suggestions of FD > 0.15–0.2 mm (Power et al., 2014). After removal of motion-corrupted runs, all subjects had at least two valid fMRI runs. Correlation values in corresponding edges were finally averaged across valid runs to obtain a single FC matrix per subject. The subjects included in the sample were not found to be significantly different in terms of motion content as function of the archetype. Inter-run and inter-subject global variability was removed by normalization (Geerligs et al., 2017).

ROI analysis on DDT and reward. Importantly, we performed a region of interest (ROI) analysis in the three groups of subjects based on a-priori hypotheses of cortical and subcortical regions recruited during the DDT and associated with reward processing (Liu et al., 2011; Li et al., 2013; Wesley and Bickel, 2014). The selected ROIs were: Ventromedial prefrontal cortex (vmPFC), orbitofrontal gyrus (OFG), middle frontal gyrus (MFG), dorsomedial prefrontal cortex (dmPFC), dorsolateral prefrontal cortex (dlPFC), superior frontal gyrus (SFG), anterior prefrontal cortex (aPFC), anterior cingulate cortex (ACC), posterior cingulate cortex (PCC), anterior internal capsule (aIC), hippocampus (Hip), parahippocampus (Parahip), Striatum, Caudatum, Putamen, Accumbens, Globus Pallidus, Thalamus, and Amygdala. These ROIs were mapped onto the cortical/subcortical parcels/regions of the Gordon-Lauman atlas according to a visual overlap criterion at the group level. The selected ROIs overlapped with 63 parcels of the 352-parcels of the Gordon-Lauman atlas extended to subcortical regions. Therefore, the initial 352 × 352 FC matrix was reduced to a 63 × 63 matrix. In general, each ROI included multiple adjacent parcels with very similar functional connectivity profiles. To enhance the statistical robustness and the interpretability of comparisons across archetypes, we averaged the correlation values of adjacent parcels within anatomically defined ROIs based on Destrieux Atlas (Fischl et al., 2002) and across hemispheres (left and right homologous parcels were averaged). This led to a reduction of the correlation matrix from 63 × 63 parcels to 18 × 18 ROIs corresponding to the functional ROIs identified above from the literature. To check that this anatomical selection was not introducing biases, we ran a hierarchical clustering on the FC profiles of the 63 parcels (Ward hierarchical method, Ward, 1963). The tree was cut to yield the same number of clusters as the anatomical areas of interest (i.e. 18). We found a high point-wise agreement (high Rand's index of 0.922; Hubert and Arabie, 1985) between the clusters and the anatomical grouping criteria.

Analysis and statistical comparisons. We carried out a Ward hierarchical clustering between coupled archetypes based on Euclidean distance similarity of connectivity profiles (i.e. FC rows, or columns by symmetry) similar to Nomi and Uddin (2015). This analysis consists in the hierarchical clustering of FC matrices to identify the node clustering structure of one group of subjects (e.g. those belonging to one archetype) and use this structure to reshape the FC representation of another group of subjects (those belonging to the other archetype). In this way, differential hierarchical organization between FC in different groups of subjects will be visually clarified. As we did not find any significant difference in the FC hierarchical organization among the three archetypes, the reported analysis is based on clustering of FC matrices based on all subjects across the three groups. Next, we tested for differences among groups using a 1-way Analysis of Variance (1w-ANOVA) with bootstrap sampling for statistic evaluation on pair-wise ROI FC (Fisher-transformed Pearson

correlations) testing the null hypothesis of equal connectivity between the three archetypes (see Xu et al., 2013; for a similar approach). An FDR method was applied to correct for not independent multiple comparisons testing conditions. Post-hoc tests were run by means of one-tailed paired two-sample *t*-test with bootstrap sampling to investigate the directionality of connectivity by archetypes couples. FDR correction was again employed and restricted according to a Bonferroni strategy over the number of performed post-hoc tests.

Software and tools. Processing of rs-fMRI data, available as Neuroimaging Informatics Technology Initiative volumes (NIFTI) or Connectivity File Based Data (CIFTI) files was done with Connectome Workbench (Marcus et al., 2011) and CARET (Van Essen Laboratory, Washington University) as well as surface visualization and representation of relevant brain areas. Statistical comparisons and further analysis were performed in MATLAB (R2016b; MathWorks, Natick, MA).

1.7. Analysis of heritability

Finally, we sought to investigate the heritability of time preferences for rewards by assessing possible differences in intra-class correlations (*r*) for the AUC $200 and AUC $40,000 between pairs of monozygotic twins (MZ; n = 130) and dizygotic twins (DZ; n = 138) by means of Fisher's z test.

Then, we calculated the heritability (h^2) index on the basis of the difference in the MZ–DZ correlations for AUC $ 200 and AUC $40,000, applying the Falconer's formula (see the study by Deary et al., 2009 for a similar approach).

2. Results

2.1. A Pareto front solution for the Delay Discounting Task (DDT)

For each participant, we took into account 25 continuous measures of the HCP (i.e., cognitive and behavioral scores), mapping them into the multi-dimensional space of traits (i.e., morphospace). The best triangular Pareto front solution was found in a two dimensional space that contains, for each subject, the values associated with the Area-under-the-curve (AUC) for $200 and AUC for $40,000, two measures of the DDT (Fig. 1). Indeed, among all possible pairwise combinations of traits, the triangle defined by the two measures of the DDT was the only one to survive the permutation test on triangularity (over 1000 permutations) corrected for False Discovery Rate (FDR) ($p < 10^{-4}$). The Principal Convex Hull/Archetypal analysis (PCHA) showed that the triangle was the best polygon to enclose all the data points among planes with 2–6 vertices. In fact, a triangle shape distribution (n = 3 vertices) explained the majority of variance (>99.5% variance), and increasing the number of vertices did not improve the amount of variance accounted for (Fig. S1 Supplementary Material).

The three vertices of the DDT triangle (identified by the colors Blue, Red, and Green, Fig. 1**)** identify *archetypes*, namely 'specialists', i.e. subjects who adopt unique strategies to deal with the discounting task, while subjects in the middle of the triangle are 'generalists'. The Blue archetype corresponds to individuals with stable preference for larger rewards that are delayed in time, independently of the amount. The Red archetype identifies individuals with stable preferences for smaller immediate rewards. The Green archetype includes individuals who prefer

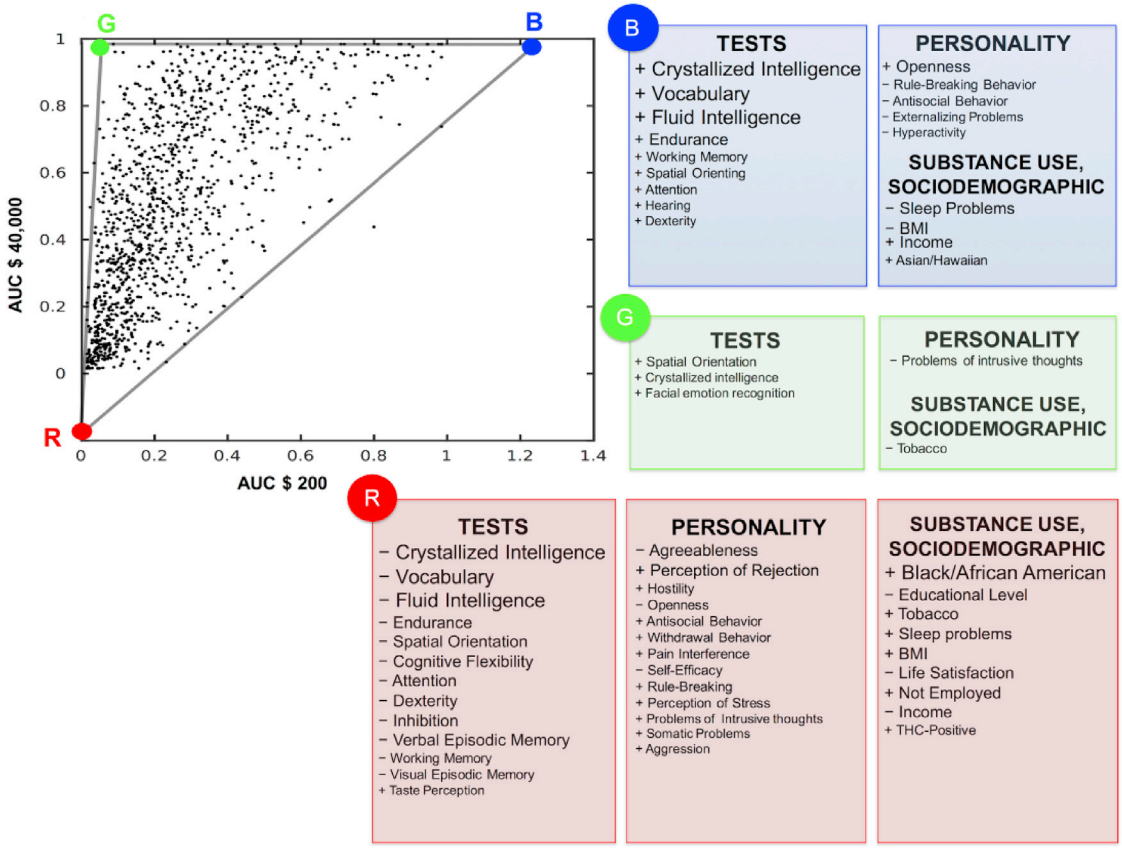

Fig. 1. Pareto distribution (triangular polytope) in a space of AUC $200 (x-axis) versus AUC $40,000 (y-axis).
The AUCs (Area-Under-the-Curve) are two measures of the Delay Discounting Task. The distribution of AUC scores is triangular hence fitting Pareto optimality theory. The three vertices of the triangle (labelled as Blue, Green, Red) contain individuals who adopt three different strategies for time preferences for reward (archetypes). These strategies co-vary with cognitive, sensory and physical abilities, personality traits, measures of substance use, and socio-demographic variables, which were identified by an enrichment analysis (see also Fig. 2 and Table 1). The size of the font corresponds to the relative significance of each trait (larger font, lower p-value).

delayed rewards when the amount is very large (i.e., $40,000), but prefer taking sooner for smaller amounts ($200).

We further validated the present results performing a split-half replication, in which the analysis was separately run on two independent group of subjects. The only significant triangle that emerged in both groups was that defined by the DDT measures (for both sub-samples: $p < 10^{-4}$, after FDR correction) (Fig. S2).

Next, we confirmed that this Pareto front distribution was independently significant in subjects of different gender ($p < 10-4$ independently for male and female subjects) and race (Asian-Native Hawaiian or Other Pacific populations: $p = 5 * 10-2$; for White subjects $p = 10^{-4}$; for Black or African American individual $p = 0.2$ (Fig. S3). In summary, the Pareto front for the DDT was highly significant, and robust over race, gender, and independent samples of subjects.

2.2. Enrichment analysis

The Pareto Front theory predicts that specialists, who adopt different strategies to solve the DDT, should show trade-offs in other cognitive tasks or in behavioral traits. To test this prediction, we employed an enrichment or density analysis. This analysis tests for systematic increases or decreases in cognitive or behavioral scores as one moves farther away from different vertices. Statistical significance was assessed by permutation tests in which the labels of the subjects belonging to each archetype were shuffled.

Cognitive, Physical and Sensory traits – We carried out the enrichment analysis on 46 features reflecting cognitive, physical, and sensory abilities from 1119 participants, with a complete data set.

We found that near the Blue archetype, several cognitive features enriched including crystallized and fluid intelligence, vocabulary knowledge, working memory, spatial orientation, and attention (Figs. 1–2; Table 1; Fig. S4). For all these measures, individuals close to the Blue archetype showed the highest scores, hence they were superior in these domains. Also measures of sensory and physical abilities enriched near/at the Blue archetype, with those subjects showing the highest levels of hearing function, submaximal cardiovascular endurance, and manual dexterity.

When focusing on the Green archetype, individuals near this vertex scored high on measures of cognitive flexibility, crystallized intelligence and spatial orientation, and were fastest in recognizing facial emotions.

Finally, individuals closest to the Red archetype showed the lowest levels of performance on crystallized and fluid intelligence, vocabulary and spatial orientation, cognitive flexibility, attention and inhibition, working memory, verbal and visual episodic memory. These individuals

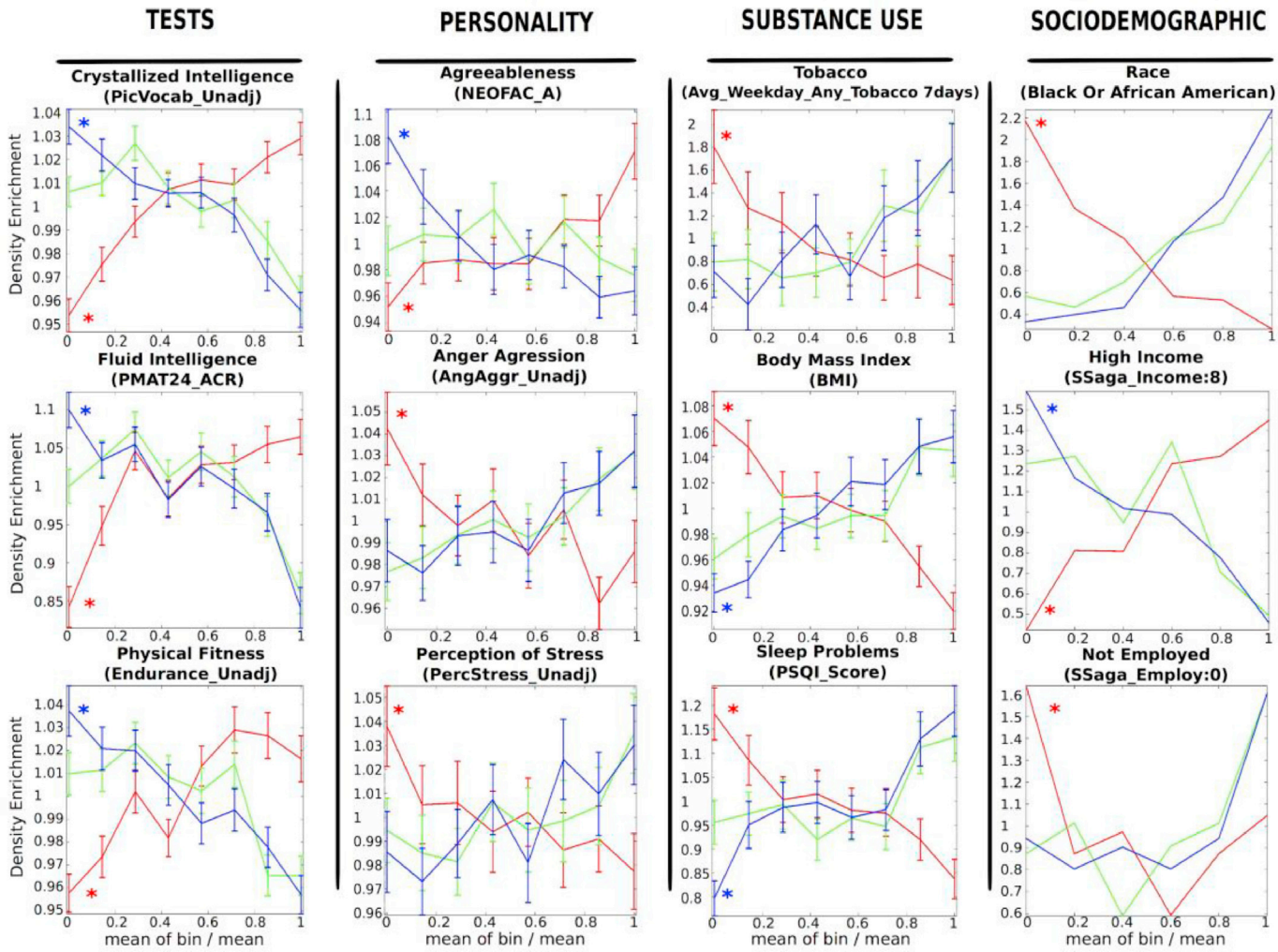

Fig. 2. Enrichment of different features near each archetype.
Individuals were binned to equal sized bins according to distance from each archetype. The average value in the bin is normalized by the average value in the whole front distribution. The error bars are computed only for continuous measures.
The enrichment analysis included cognitive tests, personality scales, substance use and socio-demographic features. Curves for features that enrich significantly near an archetype are marked with an asterisk.

Table 1
Enrichment analysis of the archetypes.
The first column represents the label of each archetype (B = Blue archetype; G = Green archetype; R = Red archetype). The second and the third columns describe the measure and the corresponding trait enriched, respectively. The resulting p-value is shown in the fourth column and it is specified, in the last column, if the value of each trait is maximum or minimum in the bin close to a given archetype. The asterisk indicates traits that are significantly enriched using a 6-bins analysis.

Archetype	Experimental Measures	Features	Average difference (p-value)	First bin
B	ReadEng_Unadj	Crystallized Intelligence	2.5873E-12	max
B	PicVocab_Unadj	Crystallized Intelligence	1.1805E-10	max
B	PMAT_ACR	Fluid Intelligence	2.9223E-10	max
B	NEOFAC_O	Openness	0.00000285	max
B	PSQI_Score	Sleep problems	0.00001369	min
B	BMI	Body Mass Index	0.0000747	min
B	Endurance_Unadj	Endurance	0.00021863	max
B	SAGA_Income: 8	High Income	0.00032978	max
B	ASR_Rule_Raw	Rule-Breaking Behaviour	0.0012588	min
B	ListSort_Unadj	Working Memory	0.001287	max
B	Race:Asian/Hawaiian/Oth Pacific	Race	0.0021611	max
B	DSM_Antis_Pct	Antisocial Behaviour	0.002465	min
B	ER40_CRT	Emotion Recognition (RTs)	0.0056397	max
B	SCPT_SPEC	Attention	0.0063268	max
B	VSPLOT_TC	Spatial Orientation	0.0077114	max
B	Noise_Comp	Hearing	0.010801	max
B	Dexterity_Unadj	Dexterity*	0.010861	max
B	ASR_Extn_Raw	Externalizing	0.013512	min
B	DSM_Hype_Raw	Hyperactivity	0.017876	min
B	Taste_Unadj	Taste*	0.037597	min
G	VSPLOT_TC	Spatial Orientation	0.0040994	max
G	ASR_Thot_Pct	Problems of intrusive thoughts	0.016071	min
G	Avg_Weeday_Any_Tobacco_7days	Tobacco	0.017359	min
G	ReadEng_Ageadj	Crystallized Intelligence	0.031099	max
G	ER40_CRT	Emotion Recognition (RTs)*	0.13533	min
R	ReadEng_Ageadj	Crystallized Intelligence	2.5873E-12	min
R	Race: Black/African American	Race	4.0364E-11	max
R	PicVocab_Unadj	Crystallized Intelligence	1.1805E-10	min
R	PMAT_ACR	Fluid Intelligence	2.9223E-10	min
R	Endurance_Unadj	Endurance	3.8829E-07	min
R	SAGA_Education: 12	Low Education	1.0987E-06	max
R	VSPLOT_TC	Spatial Orientation	2.3749E-06	min
R	SAGA_TB_Still_Smoking	Cigarette Smoking	7.5111E-06	max
R	Avg_Weeday_Any_Tobacco_7days	Tobacco	0.00001353	max
R	PSQI_Score	Sleep problems	0.00007023	max
R	CardSort_Unadj	Cognitive Flexibility	0.00012633	min
R	SCPT_SPEC	Attention	0.00021717	min
R	NEOFAC_A	Agreeableness	0.00029454	min
R	BMI	Body Mass Index	0.00031656	max
R	LifeSatisf_Unadj	Life Satisfaction	0.00035019	min
R	Flanker_Unadj	Attention/inhibition	0.00041816	min

R	SAGA_Employ: 0	Not Employed	0.00042451	max
R	SAGA_Income: 1	Low Income	0.00077582	max
R	Dexterity_Unadj	Dexterity*	0.00080057	min
R	PercReject_Unadj	Perception of Rejection	0.00090289	max
R	IWRT_TOT	Verbal episodic memory	0.00090433	min
R	THC: True	THC-positive	0.0010352	max
R	ListSort_Unadj	Working Memory	0.0012108	min
R	AngHostil_Unadj	Anger Hostility	0.0026881	min
R	DSM_Anxi_Raw	Anxiety	0.0031224	max
R	PicSeq_Unadj	Visual episodic memory	0.0032963	min
R	NEOFAC_O	Openness	0.0045872	min
R	DSM_Antis_Raw	Antisocial Behaviour	0.005532	max
R	ASR_Witd_Pct	Withdrawal Behaviour	0.0064302	max
R	PainInterf_Tscore	Pain interference	0.0070997	max
R	Selfeff_Unadj	Self-efficacy	0.0076984	min
R	ASR_Rule_Raw	Rule-Breaking Behaviour	0.007751	max
R	PercStress_Unadj	Perception of Stress	0.0078439	max
R	ASR_Thot_Raw	Problems in intrusive thoughts	0.011022	max
R	AngAggr_Unadj	Anger Aggression	0.011784	max
R	DSM_Somp_Raw	Somatic problems	0.012219	max
R	ASR_Oth_Raw	Other problems	0.017609	max
R	Taste_Unadj	Taste*	0.031563	max

also manifested the lowest performance on endurance and dexterity tasks. However, they scored highest on taste perception, i.e. they had a stronger perceived intensity to gustatory stimuli.

Therefore, individuals near the Red archetype showed an overall lower *g* factor. Notably, many of the cognitive, physical, sensory traits (excluding taste perception) reached a minimum near the Red archetype, and increased rapidly with distance from that archetype.

Personality, Substance use, socio-demographic traits – Data from 1123 participants were analyzed. Two analyses were performed separately on 70 continuous and 40 discrete measures (however, for clarity they will be described jointly).

The enrichment analysis was carried out on measures clustered into: (1) self-reported measures reflecting behavioral, social, and emotional problems, adaptive functioning, and substance use (e.g., ASR and DSM-oriented measures); (2) substance use and physiological variables (e.g., quality of sleep, smoking); (3) socio-demographic features (i.e., educational level, race, income) (Figs. 1–2; Table 1; Fig. S5).

Individuals closest to the Blue archetype resulted more open to experiences, defined as an appreciation for art, creativity, intellectual curiosity, and preference for variety and novelty. They also reported the lowest scores on scales related to sleep problems, rule-breaking and antisocial behavior, hyperactivity and externalizing behaviors (such as impulsivity and aggression). Finally, they had the lowest Body Mass Index (BMI), a measure of body fat.

Individuals close to the Green archetype were characterized by minimum scores in thought problems (i.e., hallucinations, strange thoughts and behaviors, obsessive-compulsive behavior, self-harm and suicide attempts), and by the lowest number of cigarette smoked per day (or other tobacco-related substances (Table 1; Fig. S5)).

Finally, near the Red archetype, several features enriched with maximum scores in scales reflecting aggressive, hostile, antisocial and rule-breaking behavior, withdrawn behavior and anxiety. Furthermore, individuals closest to the Red archetype reported the lowest life satisfaction, highest perception of stress, most feelings of social rejection, most somatic complaints, most problems related to intrusive thoughts, greatest interference of pain perception in daily life, and poorest sleep quality. Near this archetype, we also observed the highest number of smokers, individuals reporting to smoke the most cigarettes per day, and cannabis users as indicated by the number of positive cases to the THC drug test on the day of the experiment (Figs. 1–2). Notably, BMI (obesity) was also maximal in the bin next to the Red archetype, and steeply declined with distance from that archetype.

Examining socio-demographic variables, individuals close to the Blue archetype had the highest income whereas individuals close to the Red archetype had the lowest income, lower educational level, and were most frequently unemployed.

Finally, when considering enrichment on the variable race, Black or African-American individuals were more numerous near the Red archetype, whereas Asian (and Hawaiian or other Pacific Islanders) individuals were more concentrated in the bin closest to the Blue archetype (Fig. 2). The variable race was one of the strongest enriched features ($p = 4.06 \times 10^{-11}$). Therefore, it is important to ask whether a triangular distribution for the DDT scores existed separately in each race. As shown above (Fig. S3), a Pareto optimal distribution was found in each racial group, i.e. when considering separately White, Asian and Hawaiian individuals, or Blacks. In Black subjects, however, the distribution was also triangular, but no longer significant, compatible with the results of the enrichment analysis (see Fig. S3).

In summary, this enrichment analysis shows that stronger (Blue archetype) and more flexible (Green archetype) self-control, as indexed by the DDT scores, are associated with higher fitness on cognitive, behavioral, socio-economic, and health variables, while weaker self-control is associated with lower scores. Importantly, Blue and Green archetype subjects scored highest on different domains, suggesting different cognitive profiles (Fig. 2 and Table 1).

2.3. Structural variables

We examined 56 measures related to mean volume of both white and gray matter, both in specific anatomical brain regions, and in the total cortical and subcortical gray and white matter level, normalized per intracranial volume. Measures were collected from a total of 1105 participants.

Only total cortical gray matter volume was shown to be significantly enriched near the archetypes. Total cortical gray matter volume was highly enriched near the Blue archetype reaching a maximum value near that archetype (Fig. 3). To compare total gray matter volume as function of archetype, we ran an ANOVA restricted to individuals close to each of

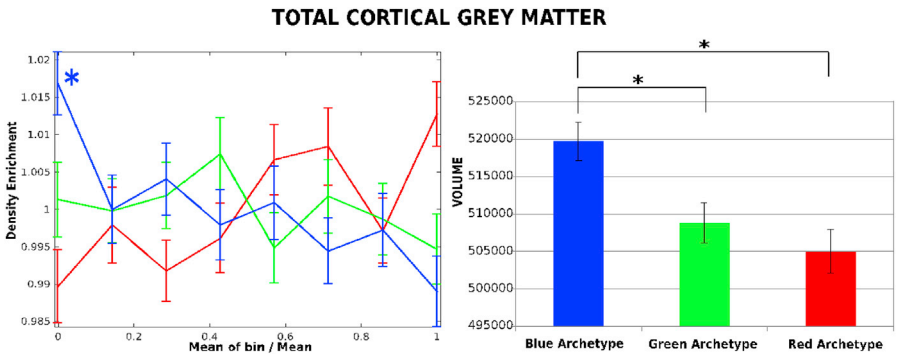

Fig. 3. Total cortical gray matter volume varies as a function of archetype.
The enrichment analysis (*left panel*) shows that total gray matter volume is enriched for the Blue archetype. The histograms (*right panel*) indicate mean volume in the sub-groups of participants (n = 100 for each group) that are closest to the three archetypes. Total cortical gray matter volume is maximal for individuals next to the Blue archetype, intermediate next to the Green archetype, and minimum next to the Red archetype. Asterisks highlight significant differences. Bars indicate standard error.

the three vertices (100 participants per group). This analysis showed a significant effect of archetype [$F(2, 297) = 7.9$; $p < 0.001$; $\eta_p^2 = 0.05$], with the Blue archetype being characterized by larger cortical gray matter volume as compared to both Red and Green archetypes ($p < 0.05$; Bonferroni correction) (Fig. 3). No difference was instead observed between Red and Green archetypes ($p > 0.05$).

In summary, stronger self-control (Blue archetype) was associated with larger gray matter volume. Importantly, Blue and Green archetype subjects showed a different profile.

2.4. Brain functional connectivity

To explore differences in functional organization we compared resting state FC to/from ROIs recruited during the DDT and associated with reward processing (Liu et al., 2011; Li et al., 2013; Wesley and Bickel, 2014) mapped onto the Gordon Laumann functional atlas of the human cerebral cortex (Gordon et al., 2014).

This analysis was run in three samples of subjects (each n = 100) who were closest to each archetype on the DDT. The three samples were matched in gender frequency (percentage of females: Red = 63%; Green = 52%; and, Blue = 57%) (Chi-square test, $p > 0.1$ for each paired comparison), and age (Average age: Red = 28.9 years old; Green = 28.6 years old; Blue = 29.6 years old) [$F(2,299) = 1.99$, $p > 0.1$], variables known to influence functional connectivity. The subjects were the same as those utilized in the structural MRI assessment.

A paired hierarchical analysis of connectivity profiles (see methods)

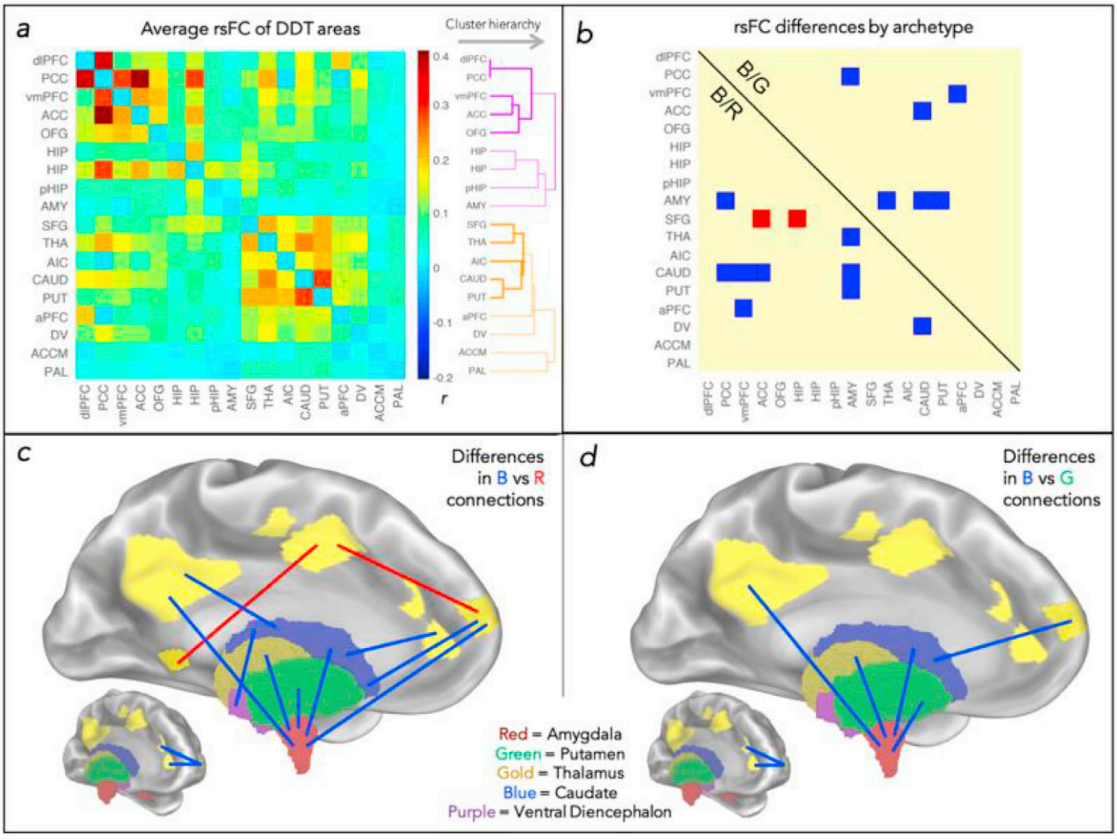

Fig. 4. Resting-state functional connectivity differences between archetypes.
(***a***) Average rsFC matrix between regions of interest involved in reward and delay discounting task. The FC matrix is divided in two clusters based on a hierarchical cluster analysis (the color indicates the same functional module membership; the thickness of the line represents the similarity of FC weighted by the connectivity significance). (***b***) Differences in rsFC among the three archetypes as identified by post-hoc comparisons. The lower triangular part compares Blue (B) versus Red (R) archetypes; the upper triangular part contrasted B archetype versus Green (G) archetype. The color of the squares indicates the edges showing stronger rsFC ($p < 0.05$, FDR corrected) for one archetype over the other.

showed two main clusters: one cluster cortical involving regions in medial prefrontal and parietal cortex plus hippocampus, parahippocampus, and amygdala; the other cluster subcortical-cortical including basal ganglia, thalamus, and lateral prefrontal cortex (Fig. 4A).

The cortical cluster (violet in Fig. 4A) includes areas belonging to the fronto-parietal network (FPN) and the default mode network (DMN), typically involved in control- and regulatory processes. The subcortical cluster (orange in Fig. 4A) includes regions more strictly related to reward processes.

To examine functional connectivity differences across archetypes, we ran a 1-way bootstrap-ANOVA with 0.05 significance level (FDR corrected for multiple comparison across 18 ROIs x17/2 tests).

Fig. 4B shows edges where FC significantly differed between archetypes: red vs. blue post-hoc comparisons under the diagonal, and blue vs. green above the diagonal of the matrix.

Interestingly, there were significant differences in ROI FC connectivity *between* clusters (Fig. 4B), specifically between prefrontal and cingulate regions, involved in control and regulation, and subcortical regions involved in reward. In contrast, there was no significant difference in ROI connectivity *within* each cluster.

In particular, subjects of the Blue archetype, as compared to subjects of the Red and Green archetypes, showed increased FC: 1) between amygdala and posterior cingulate cortex (PCC), thalamus, caudate nucleus and putamen; *2)* between caudate nucleus and ventromedial Prefrontal Cortex (vmPFC), anterior cingulate cortex (ACC), PCC, amygdala and ventral diencephalic structures (e.g., substantia nigra, hypothalamus, thalamus); and *3)* between anterior prefrontal cortex (aPFC) and vmPFC (Fig. 4B). All these connections, except those involving the amygdala, were also stronger in subjects of the Green archetype as compared to subjects of the Red archetype. The Red archetype showed stronger FC between superior frontal gyrus (SFG) and ACC and hippocampus, as compared to the other two archetypes.

In summary, stronger (blue archetype) and more flexible (green archetype) self control was associated with stronger FC between reward/emotion related regions (e.g. amygdala, caudate) and control related regions.

2.5. Twin correlations and heritability

In the last analysis, we explored the genetic influence on time preferences for rewards by assessing possible differences in intra-class correlations (r) for the AUC \$200 and AUC \$40000 between pairs of MZ twins and DZ twins by means of Fisher's z test.

The correlation value did not significantly differ between MZ and DZ pairs, either for the AUC \$200 (MZ $r = 0.30$ *versus* DZ $r = 0.32$; $z = -0.208$ $p = 0.48$), or the AUC \$40,000 (MZ $r = 0.51$ *versus* DZ $r = 0.40$; $z = 1.158$ $p = 0.124$).

The difference in MZ–DZ correlation for AUC \$ 40,000 was 0.11, indicating a broad heritability (h^2) of only 0.22. For \$AUC 200, this calculation was even meaningless as the value for DZ twins was higher than the value for MZ twins. Therefore, MZ twins were not substantially more similar in delay discounting than DZ twins. The heritability (h^2) value indicates that there is not a strong genetic dominance of this trait, as genetic dominance can be inferred for DZ twin correlations that are about ¼ MZ twin correlations.

3. Discussion

In the present study we applied Pareto Optimality theory to human cognition and behavioral data to find trade-offs and archetypes that represent potentially different evolutionary strategies in cognitive development. In the HCP dataset that measures in a large sample of healthy subjects, cognitive, sensory and physical abilities, personality traits, substance use, and socio-demographic variables, the strongest Pareto Front solution was found when we projected scores from two measures of the DDT that measures time preferences for reward, an index of self-control and regulation. This Pareto Front triangular distribution was robust in independent samples of subjects. The archetypes defined different strategies for time preference for reward that enriched on different cognitive functions, but also physical, emotional, personality, and socio-economic variables. The archetypes also differ in total gray matter volume, and functional connectivity between subcortical reward and cortical control regulatory regions. Finally, archetypes were weakly affected by genetics.

Here, we discuss the difference between Pareto Optimality and g-factor accounts of cognitive variability, potential evolutionary pressures that led to different strategies in time preference for reward, and underlying neural correlates, which provide insights into evolution, cognition, neuroscience, psychology and economy.

3.1. Pareto Optimality vs. g-factor theories of individual variability in cognition

We focused on the Pareto front distribution related to the DDT, which appeared to be the most robust. This experiment was not designed to pitch Pareto Optimality vs. g-factor theories, but to evaluate the presence of Pareto fronts and their potential significance in human cognition and behavior. The results clearly support that there is more than bivariate relationships in human cognition, and time preference for reward appears a powerful variable that shapes many other cognitive, behavioral, and brain variables. Also, we did not test higher dimensional spaces. Clearly more work is needed, but this first report is consistent with the theory that cognitive traits, as many other phenotypes in nature, are in trade-off.

3.2. Time preferences for reward: evolutionary perspective

The evolutionary foundation of time preference for rewards has attracted the interest of economists and biologists for many years (Rogers, 1994). The study of delay discounting and time preferences for reward originated from animal work (e.g., Rachlin and Green, 1972). This body of research has shown that animals discount rewards hyperbolically (Green et al., 2010), and that birds and rodents discount delayed rewards significantly more steeply than humans (Ainslie, 1974; Jimura et al., 2009). Interestingly, bonobos and chimpanzees - our closest living relatives - show a degree of patience not present in other species, and chimpanzees are even more willing to wait for food than humans (Rosati et al., 2007). Overall these studies support the evolutionary importance of discounting rewards as time-sensitive decisions are important for foraging and mating in their natural environment (see Gowdy et al., 2013).

In this study, we show that measurements of time preferences for reward in humans distribute according to a triangular Pareto front which, according to the theory, indicates that this trait is under evolutionary pressure.

The archetypes identified by the analysis correlate with other cognitive, physical, emotional, and socio-economic variables that should provide those specialist individuals with relative advantages from an evolutionary standpoint. People close to the Blue archetype enrich on features that are typically considered positive and desirable qualities, at least in a highly structured and modern environment. For example, being intelligent, agreeable, and open, as well as physically fit, could increase the likelihood to find a mate, as well as earning a high income could increase the offspring quality, via better nourishment and/or investment in education.

Likewise, people near the Green archetype flexibly changes the strategy according to the reward amount, suggesting, as compared to the two archetypes, a greater flexibility in adapting their behavior to environmental pressures. Also, these Green archetype individuals are best at recognizing facial expressions, which may help them in understanding others' feelings and needs.

The evolutionary advantage of people near the Red archetype is less

intuitive, but it may be explained as follows. Firstly, there may be 'evolutionary mismatch' between the environment in which we currently live and the environment in which we evolved. Therefore, a behavior that was adaptive hundreds of thousands to hundreds of years ago becomes inappropriate into our current environment (Robson and Samuelson, 2010). In some circumstances, for example, children and adolescents showing aggressive and externalizing behaviors become dominant and respected in their peer groups, whereas in other cases become unpopular or rejected (Frankenhuis and Del Giudice, 2012). Hence it is conceivable that the strategy of taking immediately irrespective of the rewards might have been more advantageous in the past to achieve social status and dominance.

Secondly, according to life history theory, time preferences are influenced by resource scarcity, mortality and uncertainty in the environment (Griskevicius et al., 2011). Delay discounting rate was found to be steepest under stressful conditions in people with low socio-educational background or poor health, all conditions in which individuals close to the Red archetype report to live (Chao et al., 2009; Griskevicius et al., 2011).

Finally, natural selection would favor individuals who made reproductive efforts sooner. In this regard, although the HCP dataset does not include such information, we expect that individuals close to the Red archetype were more likely to have their first child sooner and have a larger number of offspring. This speculation is supported by data showing that a steeper discounting rate in teenagers and young adults is associated with a range of sexual behaviors, including earlier first experience with sexual intercourse and past or current pregnancy (Chesson et al., 2006). Furthermore, if discounting rate is influenced by the expected future fitness, then living in relatively adverse circumstances (e.g., elevated risk of mortality, high stress levels, resource scarcity) makes individuals more prone to activate reproductive effort immediately (Daly and Wilson, 2005), as also apparent in other species (e.g. wasps, Roitberg et al., 1993).

As for the nature vs. nurture question: are archetypes in time preferences for reward genetically or environmentally determined? The absence of significant differences between MZ and DZ correlations and the low heritability (h^2) value indicate a weak genetic influence. Yet, genetic and cultural selection are not mutually exclusive. Heritability of time preferences is indeed not constant across lifespan. It is higher during late childhood/adolescence (Anokhin et al., 2011) and several studies found genetic polymorphisms being associated with differences in time preferences (Boettiger et al., 2007; Eisenberg et al., 2007). By contrast, heritability has less contribution in adulthood (age range of HCP participants: 22–35 years), when other factors, such as environmental stressors and/or cultural factors, could have an impact on individuals' time preferences to some extent.

A sensitive issue is the impact of evolutionary vs. socioeconomic factors in explaining the high proportion of Black and African American individuals near the Red vertex. Adverse health and socioeconomic conditions, as consistently revealed by the large amount of data collected through the NSAL (The National Survey of American Life: http://www.rcgd.isr.umich.edu/prba/nsal.htm#overview), may favor strategies that emphasize short term rewards. At the moment, however, the present findings cannot clearly disentangle biological and cultural factors.

3.3. Archetypes for time preference for reward: brain and cognitive associations

Our study demonstrates that archetypes for time preference for reward also differ in brain structure and functional connectivity. The Blue archetype has larger cortical gray matter volume respect to the other two archetypes, consistent with previously reported associations between brain volume and intelligence (Ritchie et al., 2015), or self-control, a critical function in the DDT (MacLean et al., 2014). Interestingly, in Mac Lean et al.' study the evolution of self-control was linked to absolute brain size across 36 different species (MacLean et al., 2014).

The three archetypes also differed in the functional connectivity profiles of brain regions associated with the DDT (Li et al., 2013; Liu et al., 2011; Wesley and Bickel, 2014). Individuals with more self-control showed stronger functional connections at rest between cortical prefrontal, cingulate, and parietal regions involved in control and regulation, and subcortical regions involved in reward and emotions. Importantly, functional connectivity differences between archetypes occurred in the projections that connected different modules. In previous work, stronger functional connections between modules or networks were observed when subjects went from rest to an attention demanding task, consistently with increased interactions (e.g. Spadone et al., 2015). So we can interpret our results suggesting that individuals with more self-control have more communication between regulatory control regions and reward regions.

These data are also consistent with a number of dual-system models of decision-making (e.g., Bechara, 2005; Bickel et al., 2007). These models state that decision-making underlies a relative balance of activation between two neurobiological systems (Bickel et al., 2007). An evolutionarily older impulsive system that includes limbic and paralimbic regions (amygdala, ventral pallidum, striatum, nucleus accumbens) values immediate rewards. By contrast, a more recently evolved control system that includes PFC and ACC is important for the inhibition/regulation of the impulsive system and the associated evaluation of delayed rewards. Our findings support these ideas showing that the ability of delaying a reward is associated with stronger functional coupling between regulatory cortical and reward subcortical regions, specifically amygdala and caudate.

A key area of the reward system is the amygdala, whose functional connections with putamen, caudate, and aPFC in our data (Fig. 4C–D) were strongly modulated by archetype, stronger in the Blue than Red and Green archetypes.

The amygdala is classically considered the core region for the regulation of emotions regulation (Costafreda et al., 2008), and a hub of emotion related networks (Pessoa, 2008). In line with our results, altered amygdala-centered connectivity was found in drug addicts (Sutherland et al., 2012) who show steeper discounting rates and lower self-regulation (Bickel et al., 2011). Interestingly, Sutherland et al. (2013) reported altered resting-state functional amygdala-centered connectivity in cigarette smokers during early nicotine withdrawal.

The ability of self-control and postpone a reward may be the result of a stronger functional connections to/from the caudate nucleus. Fronto-striatal circuitry is implicated in inhibitory control (Ghahremani et al., 2012), with the caudate nucleus associated to behavioral control and goal-directed actions (Grahn et al., 2008). Importantly, Goldstein and Volkow (2011) documented that connections between dorsal caudate and frontal regions facilitate self-control. The increased FC between caudate and PFC regions in subjects able to exert stronger self-control is consistent with these findings. Conversely, alterations of cortico-striatal connectivity have been linked to disruption of self control. Several studies have reported alteration of functional connectivity between ACC and striatum in cigarette smokers (Hong et al., 2009; Li et al., 2017), as well as altered activation of these regions in cannabis users (Yanes et al., 2018). Hong et al. (2009) have proposed that rsFC between dACC and striatum may represent a circuit-level biomarker for nicotine addiction.

The Red archetype showed stronger functional connections between ACC and superior frontal regions. Although at a first sight this result appears counterintuitive, it is, however, consistent with a study that found stronger functional coupling in ACC-frontal circuits to be predictive of a poorer DDT performance in drug addiction, even if it is important to acknowledge that the study involved a different population, namely cocaine users (Camchong et al., 2011).

Finally, from a psychological perspective, although the present study cannot make any conclusion about causal relationships, it provides the most comprehensive overview of the associations between time preference and other individuals' attributes.

We observed that people's tendency to choose more immediate or

more delayed rewards is a crucial trait that can explain individual differences not only in cognitive abilities, but also personality traits, substance use and dysfunctional behaviors, as well as socio-demographic features. Notably, in line with previous studies, we found that a stable preference for immediate smaller rewards seems to predict a constellation of behavioral and real-life problems, including hostile, antisocial, rule-breaking and withdrawal behaviors (e.g., Fossati et al., 2004), anxiety (Rounds et al., 2007), problems of intrusive thoughts (Sohn et al., 2014), sleep problems, high levels of stress and high BMI (e.g., Chan, 2017), somatic symptoms and pain interference with daily living (Tompkins et al., 2016), and perception of rejection, low levels of life satisfaction and self-efficacy, and substance addiction (e.g., Bickel et al., 2011). Taken together, our findings support the idea that steeper discounting rates are associated with a range of impulse-control disorders and unhealthy behaviors (Bickel and Mueller, 2009; Reynolds, 2006, for reviews). Therefore, time preference appears to be a promising candidate endophenotype for multiple dysfunctional behaviors and might represent a therapeutic target for treating these disease states.

4. Limitations and future directions

A limitation of this study is that our findings have not been validated with other measures of the same construct (temporal preference for reward), and in other samples of subjects. However, the replication we present in the HCP data set indicates that these findings are robust, and significantly correlated with a set of structural and functional variables. While it would be interesting to seek the same archetypes in other populations, e.g. elderly individuals or children, it is possible that this will not be straightforward as other studies have shown that delay discounting varies with age, and we show that it is not strictly dependent on genetic factors. Replication in other healthy and pathological populations is an interesting avenue for future studies, as is the search for possible cognitive and behavioral trade-offs.

A notable point of this study is the importance of moving away from bilinear correlation toward more complex models of human behavior and cognition.

Contribution

MC, AM, and GC developed the study concept. All authors contributed to the study design. LK and AP performed the data analysis. GC, LK, AM, and MC interpreted the data. GC drafted the article. MC, LK, AB, AP, and AM provided revisions. LK drafted the Supplementary Files. All authors approved the final version of the article for submission.

Acknowledgements

This study was supported by a grant from the University of Padova: PROGETTO STRATEGICO “FC-NEURO” (N°: STPD114NY2) to M.C., and from the financial support of Fondazione Cariparo.

Appendix A. Supplementary data

Supplementary data to this article can be found online at https://doi.org/10.1016/j.neuroimage.2018.10.050.

The ‘***c*** and ***d***’ panels depict the topography of significantly different connections. Connections are coloured according to the archetype that shows stronger connectivity level, separately for B/R comparison (c panel) and B/G comparison (d panel). Cortical regions are displayed in yellow, while subcortical regions are displayed according to the color legend.

References

Ainslie, G., 1974. Impulse control in pigeons. J. Exp. Anal. Behav. 21, 485–489.
Anokhin, A.P., Golosheykin, S., Grant, J.D., Heath, A.C., 2011. Heritability of delay discounting in adolescence: a longitudinal twin study. Behav. Genet. 41, 175–183.
Austin, E.J., Deary, I.J., Whitemen, M.C., Fowkes, F.G.R., Pedersen, N.L., Rabbitt, P., McInnes, L., 2002. Relationship between ability and personality: does intelligence contribute positively to personal and social adjustment? Pers. Indiv. Differ. 32, 1391–1412.
Bechara, A., 2005. Decision making, impulse control and loss of willpower to resist drugs: a neurocognitive perspective. Nat. Neurosci. 8, 1458–1463.
Bickel, W.K., Mueller, E.T., 2009. Toward the study of trans-disease processes: a novel approach with special reference to the study of co-morbidity. J. Dual Diagnosis 5 (2), 131–138. https://doi.org/10.1080/15504260902869147.
Bickel, W.K., Miller, M.L., Yi, R., Kowal, B.P., Lindquist, D.M., Pitcock, J.A., 2007. Behavioral and neuroeconomics of drug addiction: competing neural systems and temporal discounting processes. Drug Alcohol Depend. 90, S85–S91.
Bickel, et al., 2011. Remember the future: working memory training decreases delay discounting among stimulant addicts. Biol. Psychiatry 69, 260–265.
Bioucas-Dias, J.M., 2009. A variable splitting augmented Lagrangian approach to linear spectral unmixing. In: Hyperspectral Image and Signal Processing: Evolution in Remote Sensing, 2009. WHISPERS'09. IEEE, pp. 1–4. First Workshop on.
Boettiger, C.A., et al., 2007. Immediate reward bias in humans: fronto-parietal networks and a role for the catechol-O-methyltransferase 158(Val/Val) genotype. J. Neurosci. 27, 14383–14391.
Camchong, J., MacDonald, A.W., Nelson, B., Bell, C., Mueller, B.A., Specker, S., Lim, K.O., 2011. Frontal hyperconnectivity related to discounting and reversal learning in cocaine subjects. Biol. Psychiatry 69, 1117–1123.
Carroll, J.B., 1993. Human Cognitive Abilities. Cambridge Univ. Press, Cambridge.
Chan, W.S., 2017. Delay discounting and response disinhibition moderate associations between actigraphically measured sleep parameters and body mass index. J. Sleep Res. 26 (1), 21–29.
Chao, L.W., Szrek, H., Pereira, N.S., Pauly, M.V., 2009. Time preference and its relationship with age, health, and survival probability. Judgm. Decis Mak. 4 (1), 1.
Chesson, H.W., Leichliter, J.S., Zimet, G.D., Rosenthal, S.L., Bernstein, D.I., Fife, K.H., 2006. Discount rates and risky sexual behaviors among teenagers and young adults. J. Risk Uncertain. 32 (3), 217–230.
Colom, R., Jung, R.E., Haier, R.J., 2006. Distributed brain sites for the g-factor of intelligence. Neuroimage 31, 1359–1365.
Costafreda, S.G., Brammer, M.J., David, A.S., Fu, C.H.Y., 2008. Predictors of amygdala activation during the processing of emotional stimuli: a meta-analysis of 385 PET and fMRI studies. Brain Res. Rev. 58 (1), 57–70. https://doi.org/10.1016/j.brainresrev.2007.10.012.
Daly, M., Wilson, M., 2005. Carpe diem: adaptation and devaluing the future. Q. Rev. Biol. 80 (1), 55–60.
Deary, I.J., Johnson, W., Houlihan, L.M., 2009. Genetic foundations of human intelligence. Hum. Genet. 126, 215–232.
Eisenberg, D.T., MacKillop, J., Modi, M., Beauchemin, J., Dang, D., Lisman, S.A., et al., 2007. Examining impulsivity as an endophenotype using a behavioral approach: a DRD2 TaqI A and DRD4 48-bp VNTR association study. Behav. Brain Funct. 3 (1), 2.
Fischl, B., Salat, D.H., Busa, E., Albert, M., Dieterich, M., Haselgrove, C., et al., 2002. Whole brain segmentation: automated labeling of neuroanatomical structures in the human brain. Neuron 33 (3), 341–355.
Floyd, R.G., Shands, E.I., Rafael, F.A., Bergeron, R., McGrew, K.S., 2009. The dependability of general-factor loadings: the effects of factor-extraction methods, test battery composition, test battery size, and their interactions. Intelligence 37 (5), 453–465.
Fossati, A., Barratt, E.S., Carretta, I., Leonardi, B., Grazioli, F., Maffei, C., 2004. Predicting borderline and antisocial personality disorder features in nonclinical subjects using measures of impulsivity and aggressiveness. Psychiatr. Res. 125 (2), 161–170.
Frankenhuis, W.E., Del Giudice, M., 2012. When do adaptive developmental mechanisms yield maladaptive outcomes? Dev. Psychol. 48 (3), 628.
Gallagher, T., Bjorness, T., Greene, R., You, Y.J., Avery, L., 2013. The geometry of locomotive behavioral states in C. elegans. PloS One 8 (3), e59865.
Geerligs, L., Tsvetanov, K.A., Henson, R.N., 2017. Challenges in measuring individual differences in functional connectivity using fMRI: the case of healthy aging. Hum. Brain Mapp. 38 (8), 4125–4156.
Ghahremani, D., Lee, B., Robertson, C., Tabibnia, G., Morgan, A., De Shetler, N., Brown, A., Monterosso, J., Aron, A., Mandelkern, M., Poldrack, R., London, E., 2012. Striatal dopamine d2/d3 receptors mediate response inhibition and related activity in frontostriatal neural circuitry in humans. J. Neurosci. 32, 7316–7324.
Glasser, M.F., Sotiropoulos, S.N., Wilson, J.A., Coalson, T.S., Fischl, B., Andersson, J.L., et al., 2013. The minimal preprocessing pipelines for the Human Connectome Project. Neuroimage 80, 105–124.
Goldstein, R.Z., Volkow, N.D., 2011. Dysfunction of the prefrontal cortex in addiction: neuroimaging findings and clinical implications. Nat. Rev. Neurosci. 12, 652–669.
Gordon, E.M., Laumann, T.O., Adeyemo, B., Huckins, J.F., Kelley, W.M., Petersen, S.E., 2014. Generation and evaluation of a cortical area parcellation from resting-state correlations. Cer. cor. 26 (1), 288–303.
Gowdy, J., Rosser, J.B., Roy, L., 2013. The evolution of hyperbolic discounting: implications for truly social valuation of the future. J. Econ. Behav. Organ. 90, S94–S104.
Grahn, J., Parkinson, J., Owen, A., 2008. The cognitive functions of the caudate nucleus. Prog. Neurobiol. 86, 141–155.
Green, L., Myerson, J., 2004. A discounting framework for choice with delayed and probabilistic rewards. Psychol. Bull. 130 (5), 769.
Green, L., Myerson, J., Calvert, A., 2010. Pigeons' discounting of probabilistic and delayed reinforcers. J. Exp. Anal. Behav. 94, 113–123.
Griskevicius, V., Tybur, J.M., Delton, A.W., Robertson, T.E., 2011. The influence of mortality and socioeconomic status on risk and delayed rewards: a life history theory approach. J. Pers. Soc. Psychol. 100 (6), 1015.

Hart, Y., Sheftel, H., Hausser, J., Szekely, P., Ben-Moshe, N.B., Korem, Y., et al., 2015. Inferring biological tasks using Pareto analysis of high-dimensional data. Nat. Methods 12 (3), 233–235.
Hlinka, J., Paluš, M., Vejmelka, M., Mantini, D., Corbetta, M., 2011. Functional connectivity in resting-state fMRI: is linear correlation sufficient? Neuroimage 54 (3), 2218–2225.
Hong, L.E., Gu, H., Yang, Y., Ross, T.J., Salmeron, B.J., Buchholz, B., et al., 2009. Association of nicotine addiction and nicotine's actions with separate cingulate cortex functional circuits. Arch. Gen. Psychiatr. 66 (4), 431–441.
Hubert, L., Arabie, P., 1985. Comparing partitions. J. Classific. 2 (1), 193–218.
Jimura, K., Myerson, J., Hilgard, J., Braver, T., Green, L., 2009. Are people really more patient than other animals? Evidence from human discounting of real liquid rewards. Psychonomic Bull. Rev. 16, 1071–1075.
Kirby, K.N., Marakovic, N.N., 1996. Delay-discounting probabilistic rewards: rates decrease as amounts increase. Psychon. Bull. Rev. 3 (1), 100–104.
Kirby, K.N., Petry, N.M., Bickel, W.K., 1999. Heroin addicts have higher discount rates for delayed rewards than non-drug-using controls. J. Exp. Psychol. Gen. 128 (1), 78–87.
Korem, Y., Szekely, P., Hart, Y., Sheftel, H., Hausser, J., Mayo, A., Rothenberg, M.E., Kalisky, T., Alon, U., 2015. Geometry of the gene expression space of individual cells. PLoS Comput. Biol. 11 (7), e1004224.
Koçillari, L., Fariselli, P., Trovato, A., Seno, F., Maritan, A., 2018. Signature of Pareto optimization in the Escherichia coli proteome. Sci. Rep. 8 (1), 9141.
Lagorio, C.H., Madden, G.J., 2005. Delay discounting of real and hypothetical rewards III: steady-state assessments, forced-choice trials, and all real rewards. Behav. Process. 69 (2), 173–187.
Li, N., Ma, N., Liu, Y., He, X.-S., Sun, D.-L., Fu, X.-M., et al., 2013. Resting-state functional connectivity predicts impulsivity in economic decision-making. J. Neurosci. 33 (11), 4886–4895. https://doi.org/10.1523/JNEUROSCI.1342-12.2013.
Li, S., Yang, Y., Hoffmann, E., Tyndale, R.F., Stein, E.A., 2017. CYP2A6 genetic variation alters striatal-cingulate circuits, network hubs, and executive processing in smokers. Biol. Psychiatry 81 (7), 554–563.
Liu, X., Hairston, J., Schrier, M., Fan, J., 2011. Common and distinct networks underlying reward valence and processing stages: a meta-analysis of functional neuroimaging studies. Neurosci. Biobehav. Rev. 35 (5), 1219–1236. https://doi.org/10.1016/j.neubiorev.2010.12.012.
MacLean, E.L., et al., 2014. The evolution of self-control. Proc. Nat. Acad Sci. USA 111 (20), E2140–E2148.
Marcus, D.S., Harwell, J., Olsen, T., Hodge, M., Glasser, M.F., Prior, F., et al., 2011. Informatics and data mining tools and strategies for the human connectome project. Front. Neuroinf. 5.
Mobini, S., Grant, A., Kass, A.E., Yeomans, M.R., 2007. Relationships between functional and dysfunctional impulsivity, delay discounting and cognitive distortions. Pers. Indiv. Differ. 43, 1517–1528.
Mørup, M., Hansen, L.K., 2012. Archetypal analysis for machine learning and data mining. Neurocomputing 80, 54–63.
Myerson, J., Green, L., Warusawitharana, M., 2001. Area under the curve as a measure of discounting. J. Exp. Anal. Behav. 76 (2), 235–243.
Nomi, J.S., Uddin, L.Q., 2015. Developmental changes in large-scale network connectivity in autism. Neuroimage: Clin. 7, 732–741.
Pessoa, L., 2008. On the relationship between emotion and cognition. Nat. Rev. Neurosci. 9 (2), 148–158. https://doi.org/10.1038/nrn2317.
Peters, J., Büchel, C., 2011. The neural mechanisms of inter-temporal decision-making: understanding variability. Trends Cognit. Sci. 15 (5), 227–239. https://doi.org/10.1016/j.tics.2011.03.002.
Power, J.D., Mitra, A., Laumann, T.O., Snyder, A.Z., Schlaggar, B.L., Petersen, S.E., 2014. Methods to detect, characterize, and remove motion artifact in resting state fMRI. Neuroimage 84, 320–341.
Rachlin, H., Green, L., 1972. Commitment, choice and self-control. J. Exp. Anal. Behav. 17 (1), 15–22.
Reynolds, B., 2006. A review of delay-discounting research with humans: relations to drug use and gambling. Behav. Pharmacol. 17 (8), 651–667.
Ritchie, S.J., Booth, T., Hernández, M.D.C.V., Corley, J., Maniega, S.M., Gow, A.J., et al., 2015. Beyond a bigger brain: multivariable structural brain imaging and intelligence. Intelligence 51, 47–56.
Robinson, E.C., Jbabdi, S., Glasser, M.F., Andersson, J., Burgess, G.C., Harms, M.P., et al., 2014. MSM: a new flexible framework for multimodal surface matching. Neuroimage 100, 414–426.
Robson, A.J., Samuelson, L., 2010. The evolutionary foundations of preferences. In: Handbook of Social Economics, vol. 1, pp. 221–310.
Rogers, A.R., 1994. Evolution of time preference by natural selection. Am. Econ. Rev. 460–481.
Roitberg, B.D., Sircom, J., Roitberg, C.A., 1993. Life expectancy and reproduction. Nature 364, 108.
Rosati, A., Stevens, J., Hare, B., Hauser, M., 2007. The evolutionary origins of human patience: temporal preferences in chimpanzees, bonobos, and human adults. Current Biol. 17, 1663–1668.
Rounds, J.S., Beck, J.G., Grant, D.M., 2007. Is the delay discounting paradigm useful in understanding social anxiety? Behav. Res. Ther. 45 (4), 729–735.
Salimi-Khorshidi, G., Douaud, G., Beckmann, C.F., Glasser, M.F., Griffanti, L., Smith, S.M., 2014. Automatic denoising of functional MRI data: combining independent component analysis and hierarchical fusion of classifiers. Neuroimage 90, 449–468.
Sheftel, H., Szekely, P., Mayo, A., Sella, G., Alon, U., 2018. Evolutionary trade-offs and the structure of polymorphisms. Phil. Trans. R. Soc. B 373 (1747), 20170105.
Shoval, O., Sheftel, H., Shinar, G., Hart, Y., Ramote, O., Mayo, A., et al., 2012. Evolutionary trade-offs, Pareto optimality, and the geometry of phenotype space. Science 336 (6085), 1157–1160.
Smith, S.M., Miller, K.L., Salimi-Khorshidi, G., Webster, M., Beckmann, C.F., Nichols, T.E., et al., 2011. Network modelling methods for FMRI. Neuroimage 54 (2), 875–891.
Sohn, S.Y., Kang, J.I., Namkoong, K., Kim, S.J., 2014. Multidimensional measures of impulsivity in obsessive-compulsive disorder: cannot wait and stop. PloS One 9 (11), e111739.
Spadone, S., Della Penna, S., Sestieri, C., Betti, V., Tosoni, A., Perrucci, M.G., et al., 2015. Dynamic reorganization of human resting-state networks during visuospatial attention. Proc. Acad. Nat. Sci. 201415439.
Spearman, C., 1904. General intelligence, objectively determined and measured. Am. J. Psychol. 15 (2), 201–293.
Sutherland, M.T., McHugh, M.J., Pariyadath, V., Stein, E.A., 2012. Resting state functional connectivity in addiction: lessons learned and a road ahead. Neuroimage 62 (4), 2281–2295. https://doi.org/10.1016/j.neuroimage.2012.01.117.
Sutherland, M.T., Carroll, A.J., Salmeron, B.J., Ross, T.J., Hong, L.E., Stein, E.A., 2013. Down-regulation of amygdala and insula functional circuits by varenicline and nicotine in abstinent cigarette smokers. Biol. Psychiatry 74 (7), 538–546.
Szekely, P., Korem, Y., Moran, U., Mayo, A., Alon, U., 2015. The mass-longevity triangle: Pareto optimality and the geometry of life-history trait space. PLoS Comput. Biol. 11 (10), e1004524.
Tendler, A., Mayo, A., Alon, U., 2015. Evolutionary tradeoffs, Pareto optimality and the morphology of ammonite shells. BMC Syst. Biol. 9 (1), 12.
Thøgersen, J.C., Mørup, M., Damkiær, S., Molin, S., Jelsbak, L., 2013. Archetypal analysis of diverse Pseudomonas aeruginosa transcriptomes reveals adaptation in cystic fibrosis airways. BMC Bioinf. 14 (1), 279.
Tompkins, D.A., Johnson, P.S., Smith, M.T., Strain, E.C., Edwards, R.R., Johnson, M.W., 2016. Temporal preference in individuals reporting chronic pain: discounting of delayed pain-related and monetary outcomes. Pain 157 (8), 1724.
Van Essen, D.C., Smith, S.M., Barch, D.M., Behrens, T.E., Yacoub, E., Ugurbil, K., HCP Consortium, Wu-Minn, 2013. The Wu-Minn human connectome project: an overview. Neuroimage 80, 62–79.
Ward Jr., J.H., 1963. Hierarchical grouping to optimize an objective function. J. Am. Stat. Assoc. 58 (301), 236–244.
Wesley, M.B.W., Bickel, W.K., 2014. Remember the future II: meta-analyses and functional overlap of working memory and delay discounting. Biol. Psychol. 454 (1), 42–54. https://doi.org/10.1097/OPX.0b013e3182540562.
Xu, L.W., Yang, F.Q., Qin, S., 2013. A parametric bootstrap approach for two-way ANOVA in presence of possible interactions with unequal variances. J. Multivariate Anal. 115, 172–180.
Yanes, J.A., Riedel, M.C., Ray, K.L., Kirkland, A.E., Bird, R.T., Boeving, E.R., et al., 2018. Neuroimaging meta-analysis of cannabis use studies reveals convergent functional alterations in brain regions supporting cognitive control and reward processing. J. Psychopharmacol. 32 (3), 283–295.